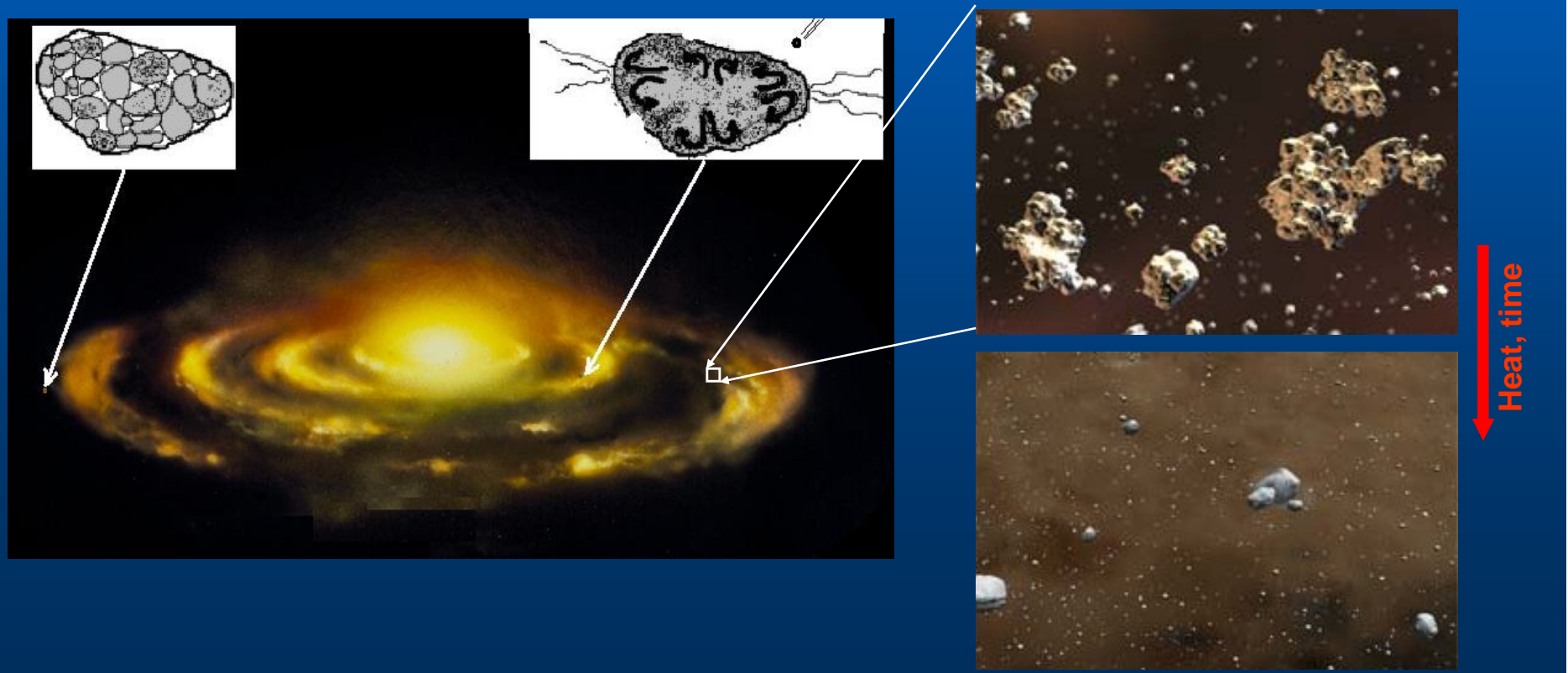


# A SIMPLE INSTRUMENT TO *IN SITU* CHARACTERIZE THE TENSILE STRENGTH OF COMETARY MATERIALS

Josep M. Trigo i Rodríguez (*Inst. Space Sciences, CSIC-IEEC*)

José M. Valverde (*Universidad de Sevilla*), &

J. Blum (*IGEP, Technische Universität Braunschweig*)

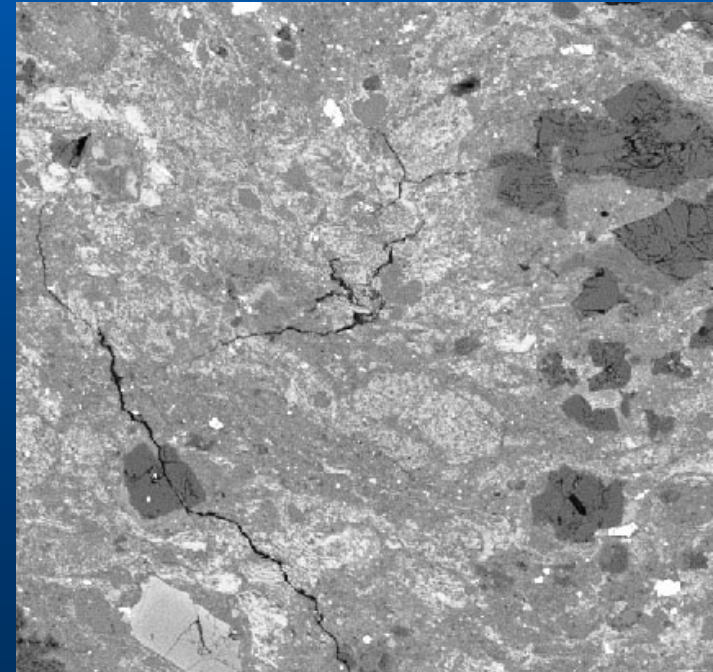


# OUTLINE

- The importance of measuring the strength
  - Tensile, shear and compressive strength: definitions
  - To what extent are minor bodies processed?
- A simple setup to put on board an exploration spacecraft:
  - Two types of materials according to their coherence:
    - Cohesive and non-cohesive
- Primitive bodies: a challenge or opportunity?
  - Obtaining tensile strengths in unprocessed bodies: meteorites and comets
  - Solar system materials preserved
- Extremely fluffy nature of cometary materials:
  - Remote determination of strengths in cometary meteoroids
  - Consistence with *Stardust* (NASA) results on comet 81P/Wild 2
- Conclusions

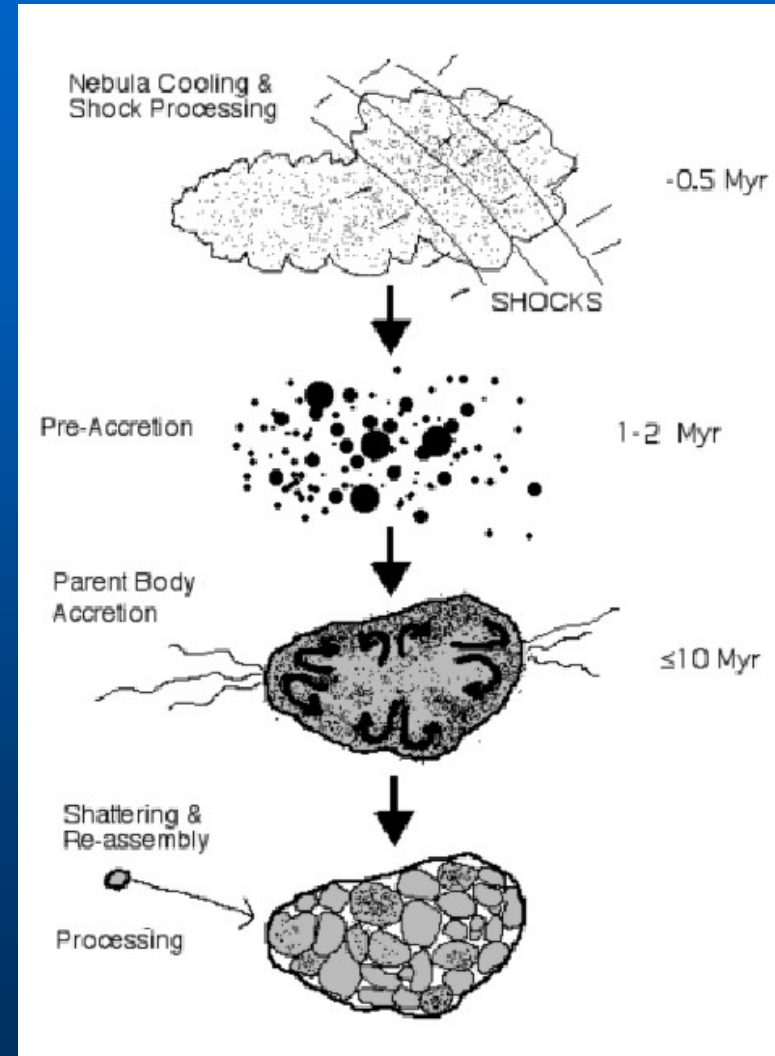
# STRENGTH: DEFINITIONS

- Generally strength is a measure of an ability to withstand stress. Three types:
  - Tensile strength ( $\sigma_t$ ) is the ability of a material to withstand uniaxial tension
  - Compressive strength ( $\sigma_c$ ): ability to withstand compressive uniaxial stress
  - Shear strength ( $\sigma_s$ ):  
ability to withstand pure shear
- Typically:  $\sigma_t > \sigma_s > \sigma_c$ 
  - $\sigma_s \sim 3 \sigma_t$  (Biele et al., 2009)
- Primitive bodies have been subjected to impacts since their formation



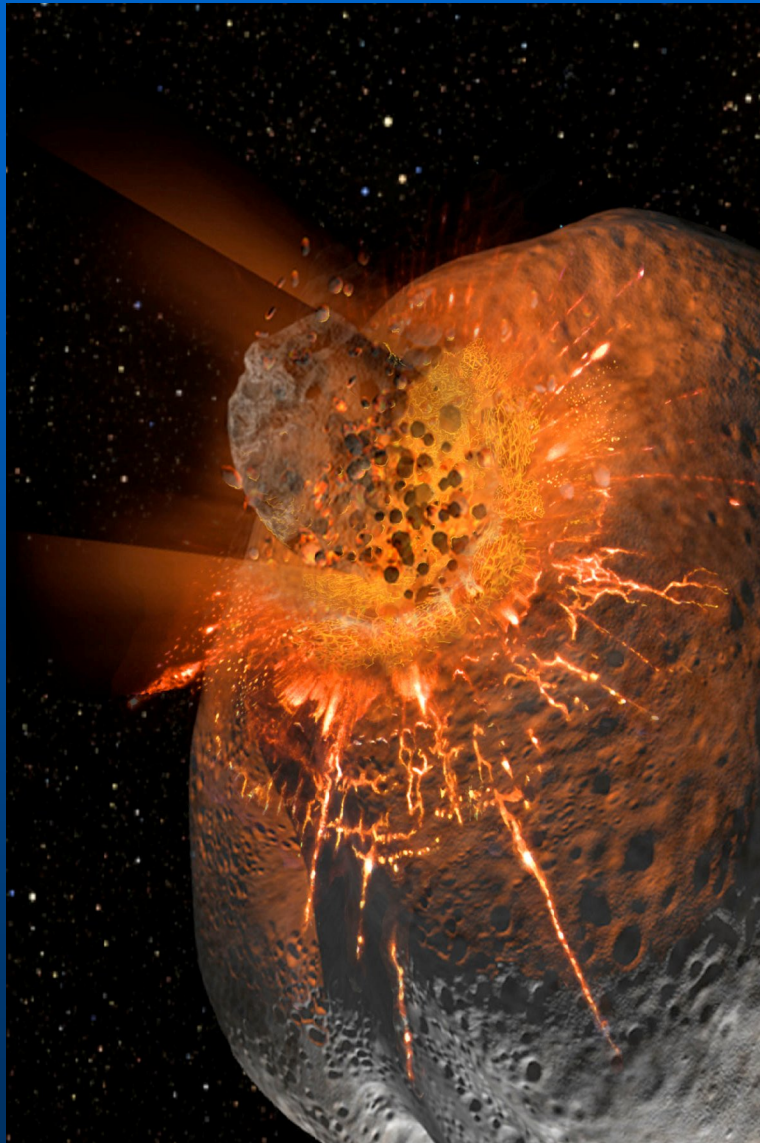
# THE FORMATION SCENARIO OF FIRST SOLAR SYSTEM MATERIALS

- **≈4.6 Gyr ago the nebula started its collapse**
  - nano to micron-sized dust arrived from nearby stars or condensed from the nebula
  - **MATERIALS INHERITED A GRANULAR STRUCTURE**
- **At ~4567 Myr: CAIs formed**
- **At ~4566 Myr: chondrule formation begins and continues for about 1-2 Myr**
- **Between 4565-4564 Myr the different components accrete to form the chondritic asteroids: first planetesimals**
- **Since then: Collisional compaction, and aqueous alteration have participated in processing the rock-forming materials of minor (undifferentiated) bodies**



Jewitt et al. (2008)

# PRIMITIVE BODIES' PROCESSING

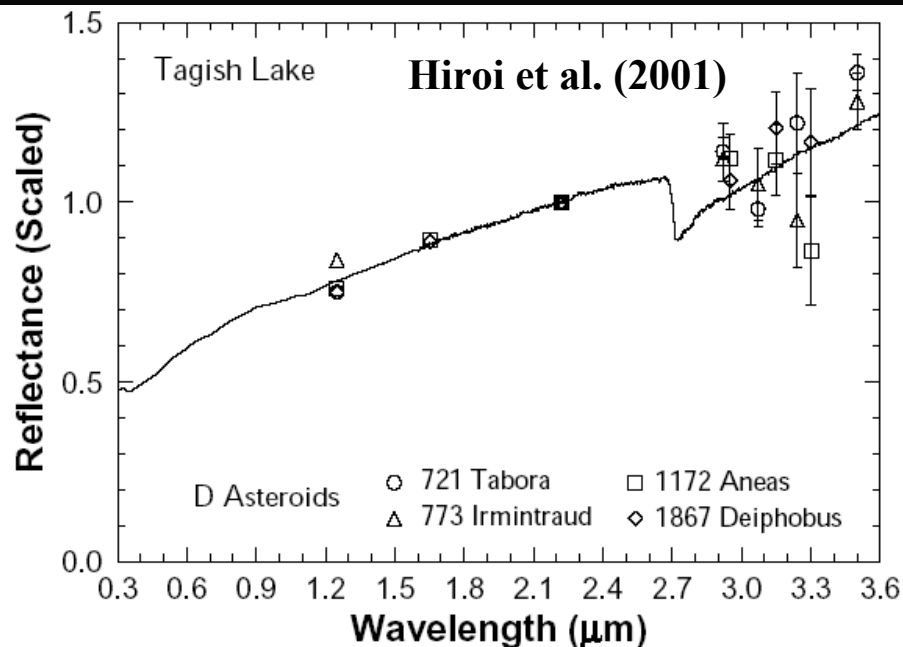


Don Dixon

- There is a huge diversity in the bulk porosity  $P$  of asteroids (Britt et al., 2002)
  - From  $P < 15\%$  Differentiated Bodies: e.g. 1 Ceres, 2 Pallas, 4 Vesta, etc...
  - $15\% < P < 50\%$ : Like e.g. 243 Ida, 433 Eros, ...
  - $P > 50\%$ . Like e.g. 22 Kalliope, 16 Pyshe, ...
- Consequences of impact processing:
  - **COMPACTION**: Porosity attenuates the stress wave generated in an impact. Materials are heated, shocked and redistributed
  - Volatiles participate in the break up of the object, water may be released internally to soak the body, aqueous alteration can increase its coherence, etc...
  - Re-aggregation: rubble piles (Michel et al.)
- Primitive (undifferentiated) bodies should have higher degree of porosity (Trigo-Rodríguez & Blum, PSS, 2009)

# METEORITE EVIDENCE ARRIVED FROM CHONDRITIC ASTEROIDS

253 Mathilde, NEAR Shoemaker (NASA)



- Chondritic meteorites are coming from undifferentiated bodies:
  - They contain chondrules, refractory inclusions, but also fine dust and organics in the matrix
- 14 chondrite groups have been identified (see e.g. Weisber et al., 2006)
- Chemical differences suggest that each group represents rocks from a different reservoir (see eg. Hutchison, 2004)
- This idea has been reinforced because few chondrite breccias exist containing clasts from different chondrite groups (Bischoff et al, 2006)
- Primitive asteroids are covered by rubble.
  - Chondrite breccias are formed by regolith compaction under the action of impacts, and subsequent aqueous alteration

# ACFER 094 M9324

1 mm

SEM BSE image of CM-like ungrouped Acfer 094 (Trigo-Rodríguez et al., 2006)

A B C D E F G H I

1

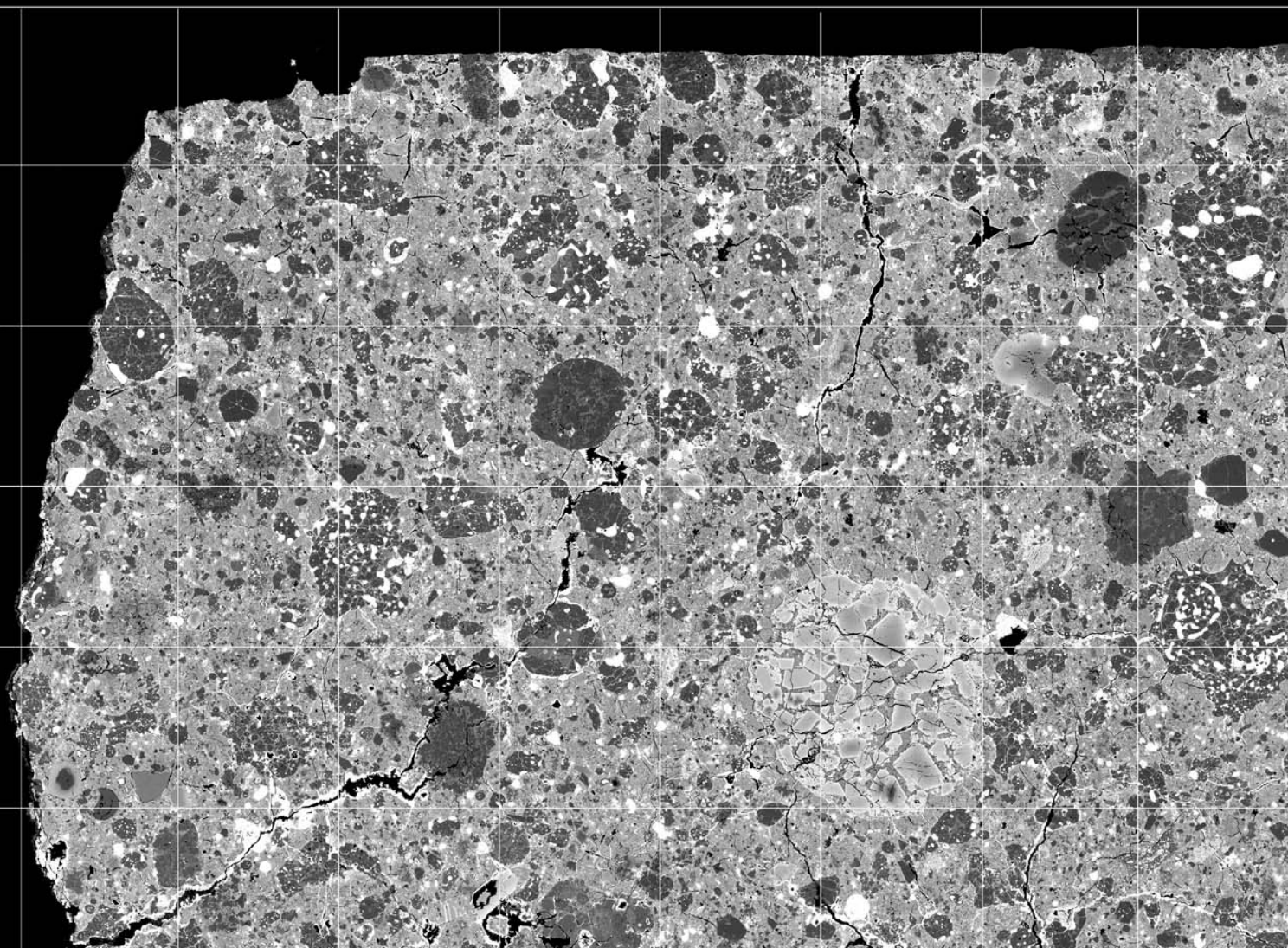
2

3

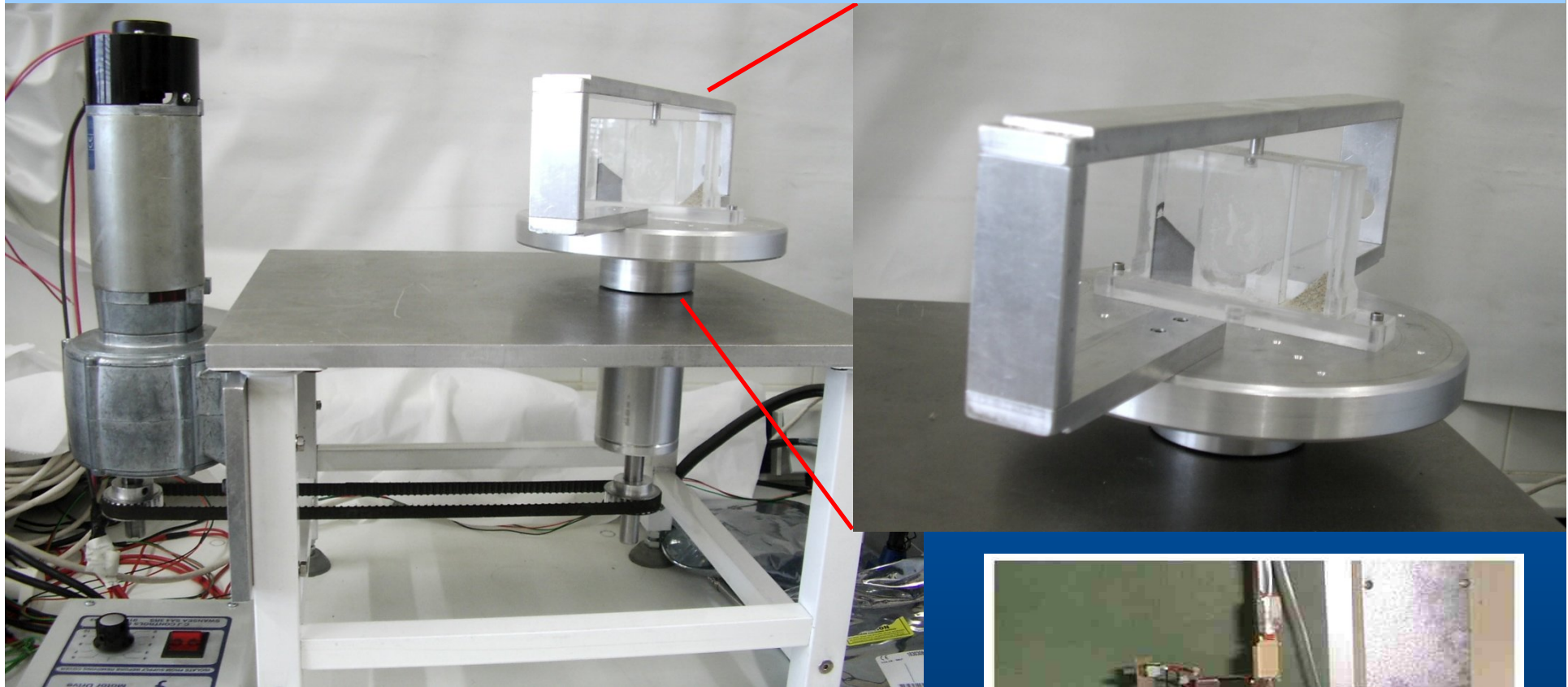
4

5

6



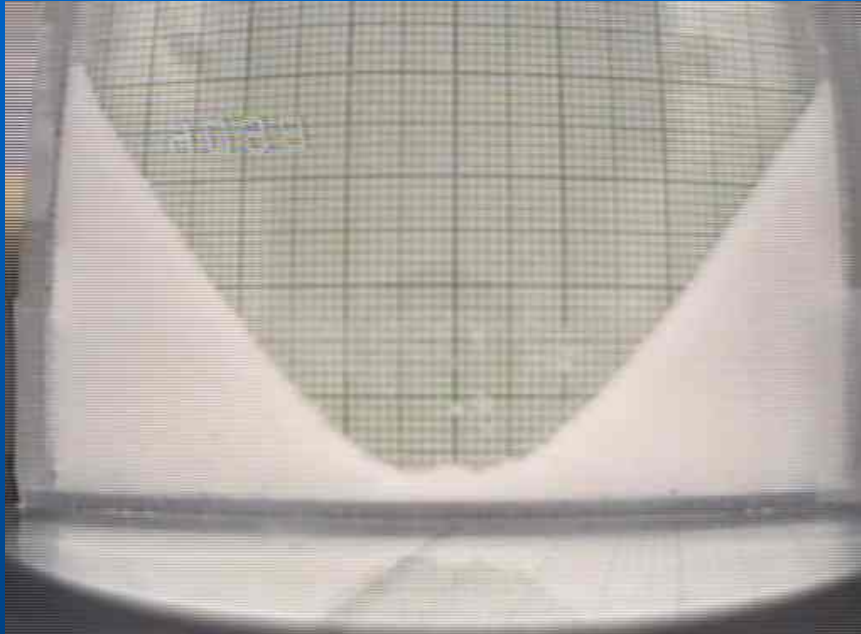
# A novel device to measure angle of internal friction and cohesion of granular materials



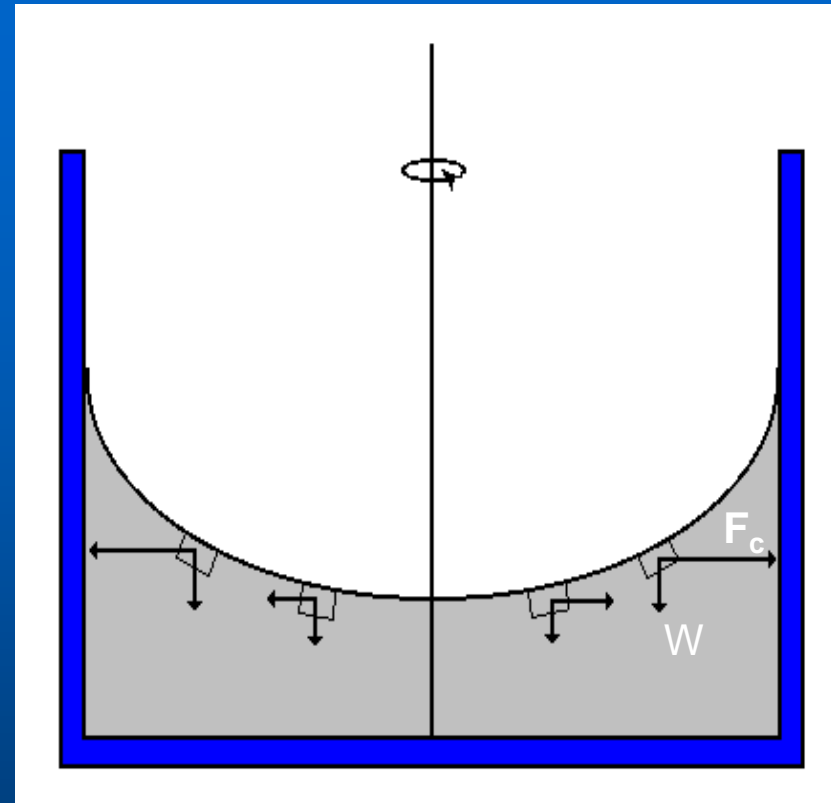
- A rectangular cell containing a sample of powder is rotated
- The centrifugal force exerts a shear stress on the sample, forcing the material to flow
- Sample is under low consolidation
- The stress state is two dimensional



# Experimental setup



500 rpm



Centrifugal force creates shear stresses causing the flow

# Classification of granular materials

Granular materials are classified in:

- Non-cohesive granular material

Characterized by an angle of internal friction  $\phi$

$\phi$  is determined by the maximum ratio between shear and consolidation stresses

- Cohesive granular material

Characterized by an angle of internal friction  $\phi$  and a cohesion  $c$

Cohesion is the shear stress the powder can withstand at zero consolidation stress

These powders show dramatic differences in flow behavior

# Two types of materials according their cohesion

## non-cohesive powder

$$\frac{\omega_0^2 \cdot R}{g} = \tan \phi$$

- Motion grain by grain, no avalanching
- The surface profile changes smoothly

## cohesive powder

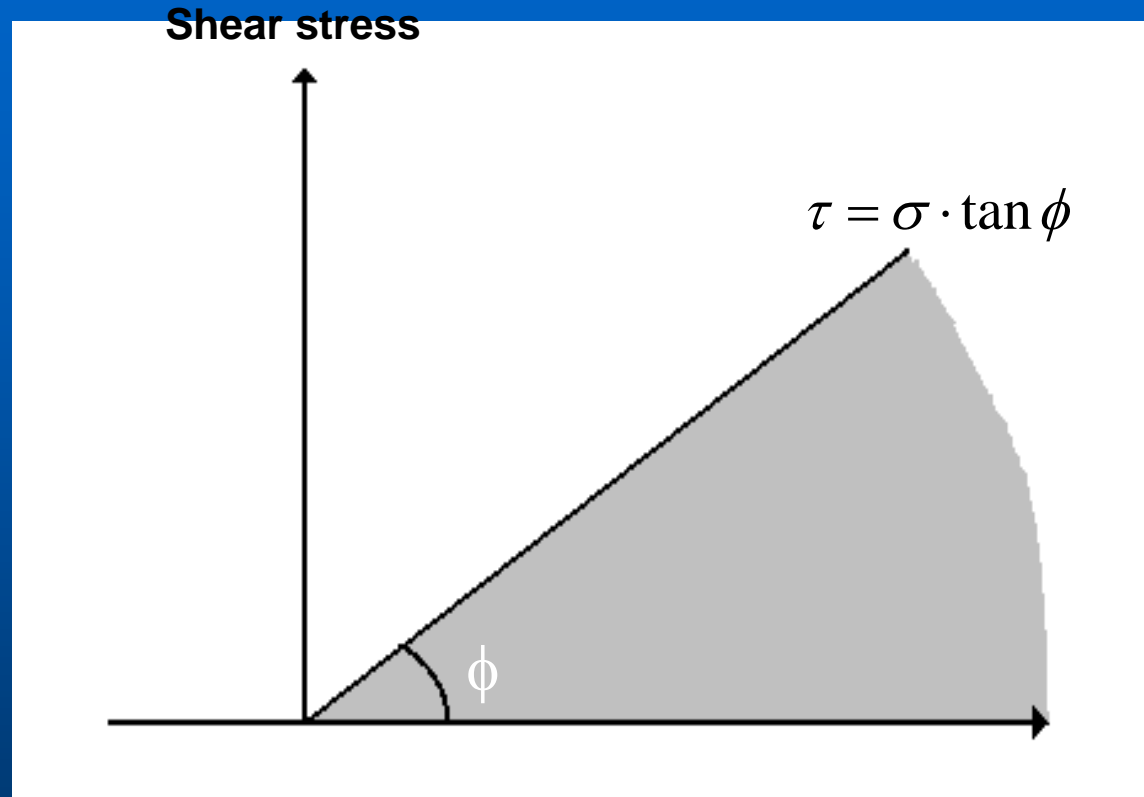
$$\frac{\omega_0^2 \cdot R}{g} > \tan \phi$$

- Powder movement takes the form of avalanches
- The surface profile changes discontinuously

Different behavior requires different models

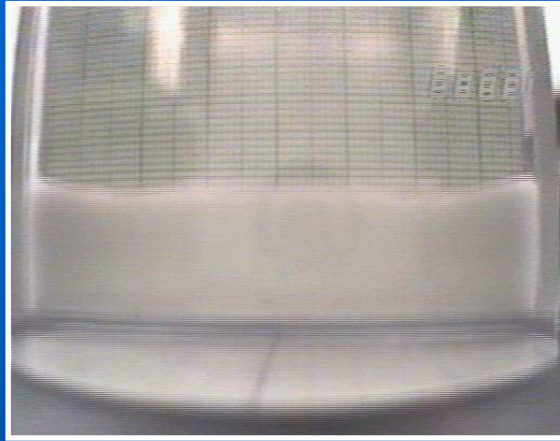
# Angle of internal friction

Coulomb yield criterion for non-cohesive powders

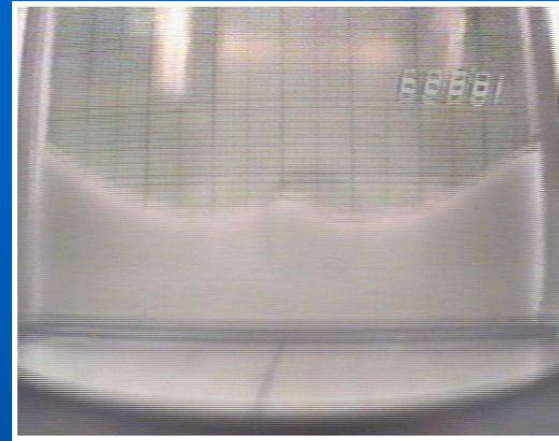


- Measures the capability of the powder to sustain shear stress
- Depends on particle shape, particle size distribution
- Only states of stress below the yield locus are possible

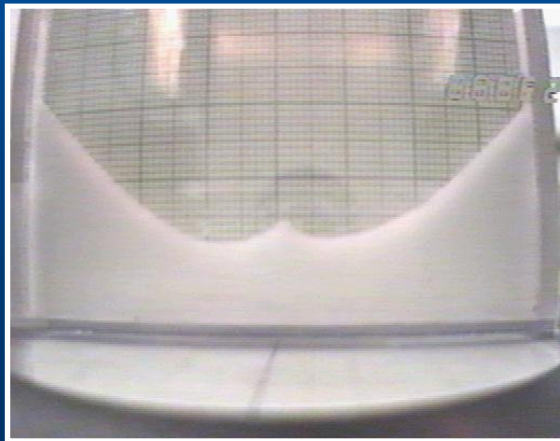
# Example: Behavior of non-cohesive powder



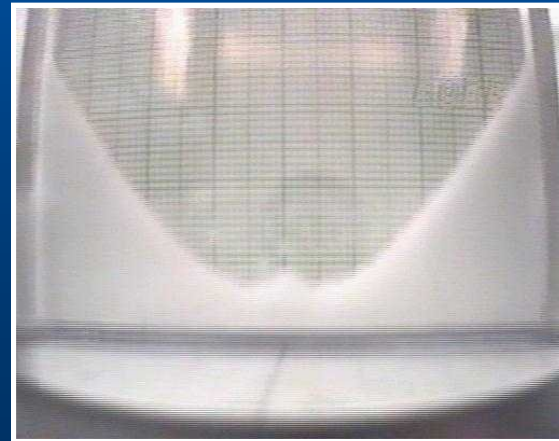
$\omega = 173$  rpm



$\omega = 251$  rpm



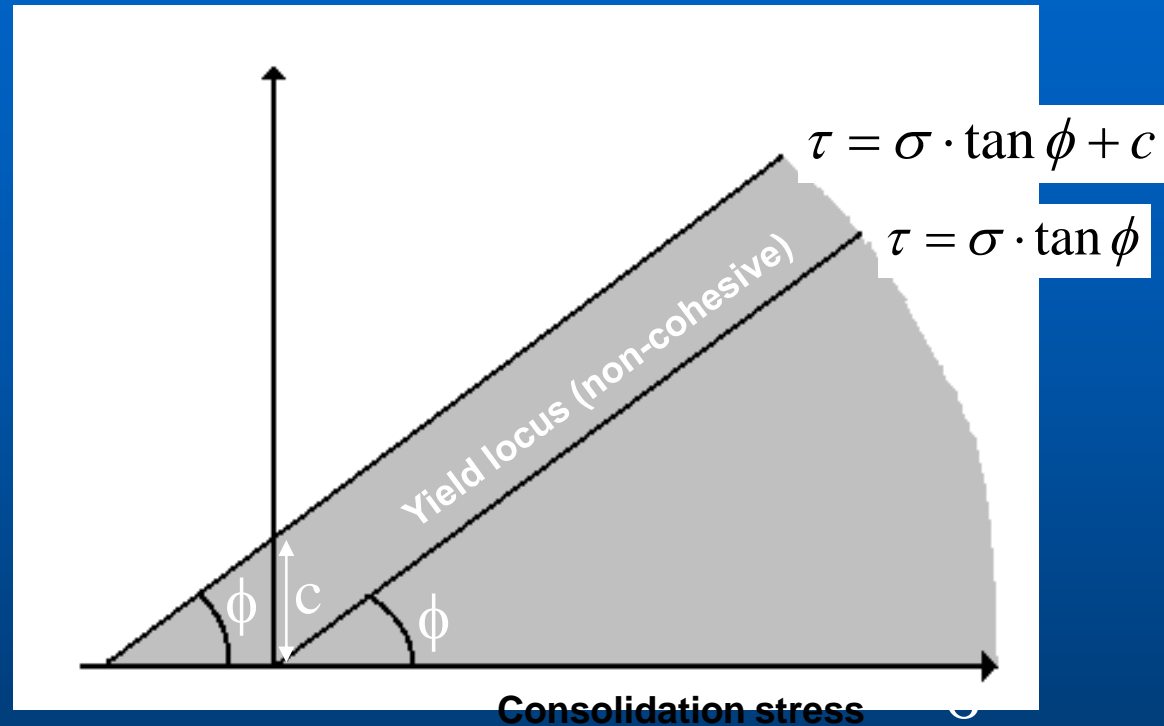
$\omega = 318$  rpm



$\omega = 520$  rpm

# Cohesion and angle of internal friction

Coulomb yield criterion for cohesive powders



- An uncompressed cohesive powder can withstand a shear stress
- Cohesion arises from interparticle forces (Van der Waals, electrostatic) and liquid bridges

# Measurement technique

- obtain  $C$  from the angular speed at which first avalanche occurs



Developer after first avalanche.

- obtain  $\phi$  from avalanches at high angular speed.



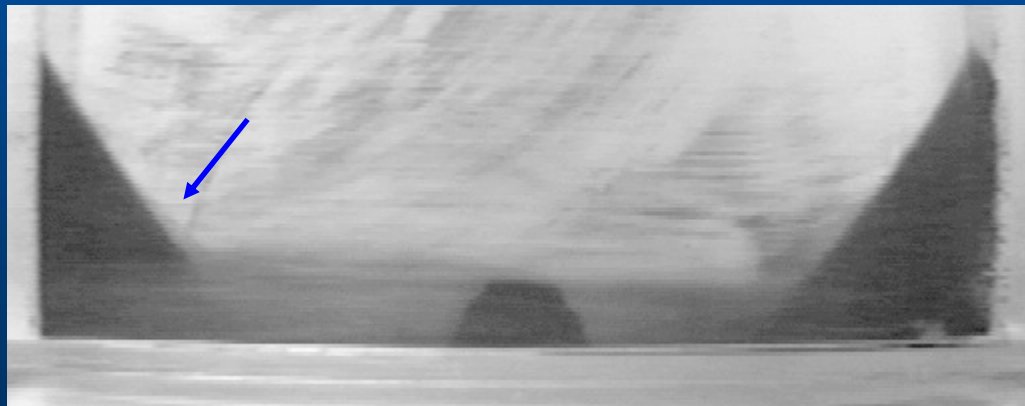
Profile of the sample at high angular speed.

# MEASUREMENT OF $\phi$ : AVALANCHING MECHANISM



- At high angular speeds the material accumulates against the cell walls forming a slope

- No avalanche is seen until the slope becomes unstable and a new, steeper slope is formed.



- This process is triggered by the increase of the angular speed

# CREATING AGGREGATES FOR TESTING STRENGTH

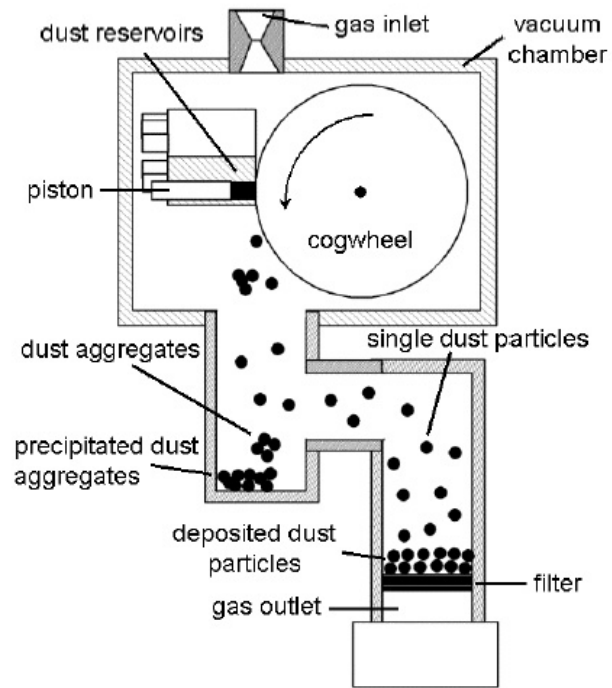
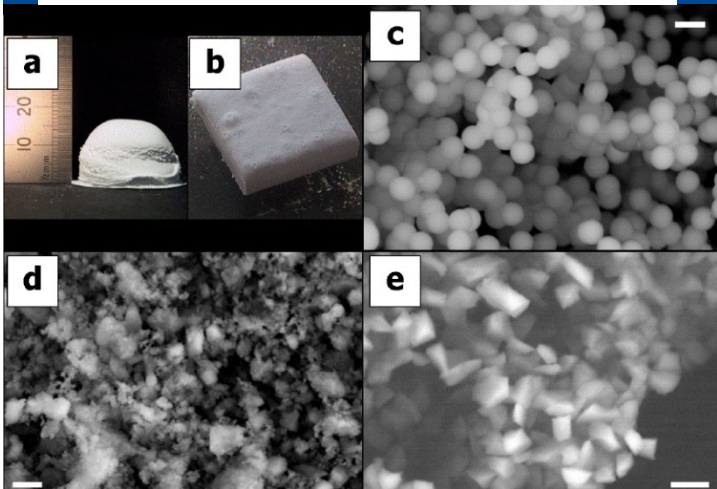


Fig. 1.— Principles of the experimental setup for the formation of macroscopic dust aggregates.

- Main goal of the experiments (Univ. Braunschweig):
  - To learn about the expected physical properties of primeval accretionary bodies
- Study of macroscopic aggregates (a,b) built from different types of grains:
  - c) Spherical monodisperse  $\text{SiO}_2$  grains
  - d) Irregular diamonds
  - e) Irregular polydisperse  $\text{SiO}_2$
- Resulting porosities of the order of 80 to 67% for the maximum compression of planetesimals (relative velocities of 50 m/s)
- Tensile strengths in the range of 0.2 to 1.1 kPa



Blum et al., ApJ (2006)

Tensile  
Strength  
Determination  
experiment



# CLUES FROM METEORITES' POROSITY

- Chondrite meteorites arrived to Earth's surface are compacted samples (!):
  - They are biased during release, interplanetary travel, and entry towards the tougher objects

MEASURED AND MODELLED POROSITIES AND BULK DENSITIES FOR PRIMITIVE METEORITES (CCs AND ORDINARY) COMPARED TO OTHER PROCESSED METEORITES (ACHONDRITES, ENSTATITE AND STONY-IRON). ONLY THOSE METEORITE GROUPS WITH A REPRESENTATIVE NUMBER OF MEASURED METEORITES ( $N_{\text{met}} \geq 3$ ) ARE INCLUDED. DATA FROM BRITT AND CONSOLMAGNO (2003).

Meteorite Class	Group	$N_{\text{met}}$	Average Porosity $\pi$ (%)	Bulk density (g/cm <sup>3</sup> )	
Carbonaceous chondrite	CM	18	$23.0 \pm 7.5$	$2.12 \pm 0.26$	<b>Blum et al. (2006) ApJ.</b>
Carbonaceous chondrite	CO	8	$19.8 \pm 4.1$	$2.95 \pm 0.11$	
Carbonaceous chondrite	CV	10	$13.8 \pm 9.1$	$2.95 \pm 0.26$	
Carbonaceous chondrite	CI	4	11.3	2.11	
Carbonaceous chondrite	CR	3	$6.4 \pm 3.8$	3.10	
Ordinary chondrite	H	157	$6.4 \pm 4.2$	$3.40 \pm 0.18$	
Ordinary chondrite	L	160	$4.5 \pm 4.6$	$3.35 \pm 0.16$	
Ordinary chondrite	LL	39	$7.9 \pm 4.2$	$3.21 \pm 0.22$	
Enstatite chondrite	EH	5	$-1.2 \pm 2.5$	$3.72 \pm 0.02$	
Enstatite chondrite	EL	7	2.7	$3.55 \pm 0.10$	
Achondrite	Diogenites	3	2.5	$3.26 \pm 0.17$	
Achondrite	Eucrites	9	$8.6 \pm 4.6$	$2.86 \pm 0.07$	
Achondrite	Howardites	5	$4.7 \pm 0.5$	$3.02 \pm 0.19$	
Achondrite	Aubrites	6	0	$3.12 \pm 0.15$	
Achondrite	Ureilites	3	8.9	$3.05 \pm 0.22$	
Stony-Iron	Pallasites	5	$0.0 \pm 5.2$	$4.76 \pm 0.10$	
	Mesosiderites	3	$3.0 \pm 8.1$	$4.25 \pm 0.02$	

# MORE PRISTINE OBJECTS: COMETS!

Comet SW3,  
HST (NASA)

COMETARY AND METEOROID TENSILE STRENGTHS. THE REFERENCE NUMBERS REFER TO [A] KLINGER ET AL. (1989), [B] MÖHLMANN (1996), [C] DAVIDSSON (2001), [D] LISSE ET AL. (1999), [E] TRIGO-RODRÍGUEZ AND LLORCA (2006).

Tensile strength (Pa)	Comet/Meteoroid Source	Reference
<u>Comet</u>		
10,000, > 100 ... 1,000	Sun-grazing comets	[A]
500 ± 450	46P/Wirtanen	[B]
> 3 ... 6	6P/d'Arrest	[C]
> 47	Levy 1991 XI	[C]
> 2	28P/Neujmin I	[C]
> 5	29P/Schwassmann-Wachmann 1	[C]
> 13 ... 53	29P/Schwassmann-Wachmann 2	[C]
> 6 ... 9	10P/Tempel 2	[C]
> 4 ... 7	107P/Wilson-Harrington	[C]
> 1	46P/Wirtanen	[C]
> 7,700 ... 46,000	95P/Chiron	[C]
> 20 ... 400	C/1996 B2 Huyakutake	[D]
<u>Meteoroid Source</u>		
34,000 ± 7000	2P/Encke (Taurids)	[E]
6,000 ± 300	7P/Pons-Winnecke	[E]
400 ± 100	21P/Giacobini-Zinner	[E]
22,000 ± 2,000	45P/Honda-Mrkos-Pajdusakova (Alpha Capricornids)	[E]
6,000 ± 3,000	55P/Tempel-Tuttle (Leonids)	[E]
12,000 ± 3,000	109P/Swift-Tuttle (Perseids)	[E]

Blum et al. (2006) ApJ.

- Tensile strengths have been proposed as indicators of the degree of primitiveness of minor bodies (Trigo-Rodríguez and Blum, 2009)
- Comets are among the less-processed solar system objects

# METEOROIDS TENSILE STRENGTH

Accurate meteor trajectory data can provide insight into physical properties like e.g. the dynamic strength (S)

$$S = \rho_{atm} \cdot v^2$$

- Tensile strengths measured for the break up of cometary meteoroids in the atmosphere

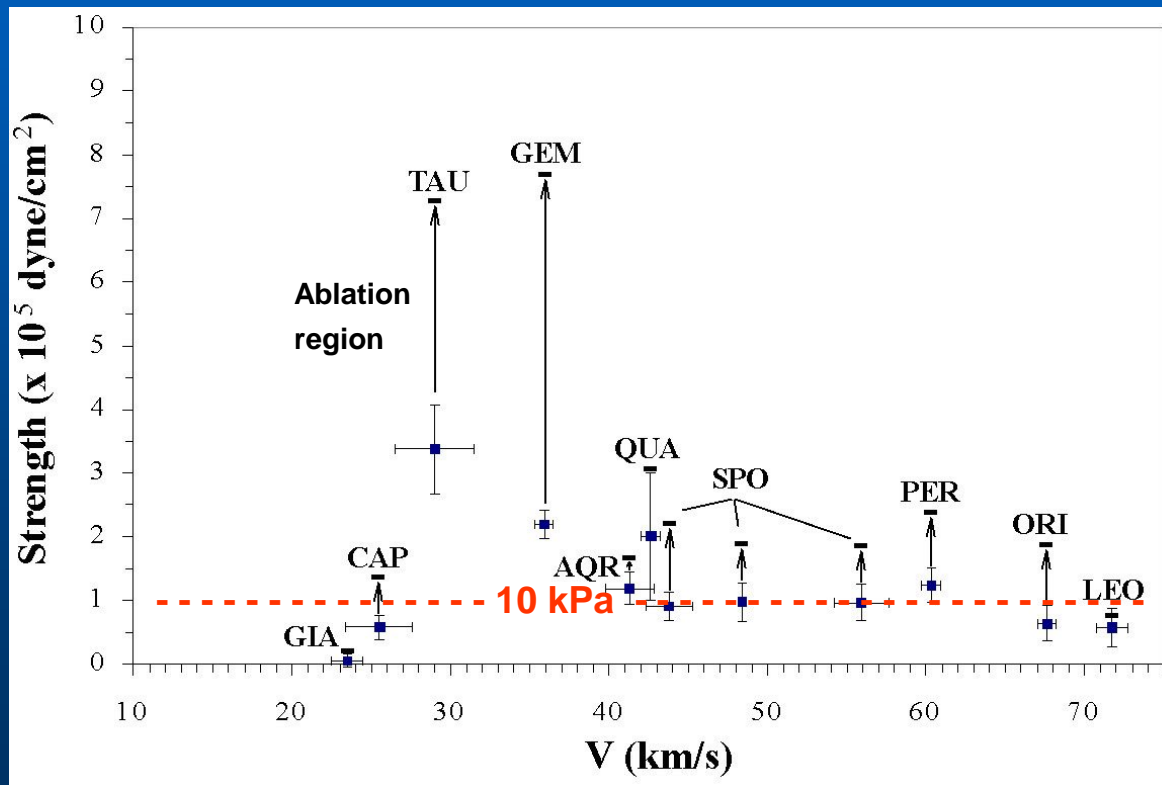
- Sporadic (SPO) particles with high entry velocities (suggesting cometary origin) have typical disruption strengths of  $10^5$  dyne/cm<sup>2</sup>.

Below this value are probably young fluffy meteoroids as for the case of CAP, LEO and ORI.

Finally GIA are exhibiting extremely low strengths.

Particles coming from old streams (TAU, GEM and QUA) associated with parent bodies exhibiting low or null cometary activity have the highest strengths.

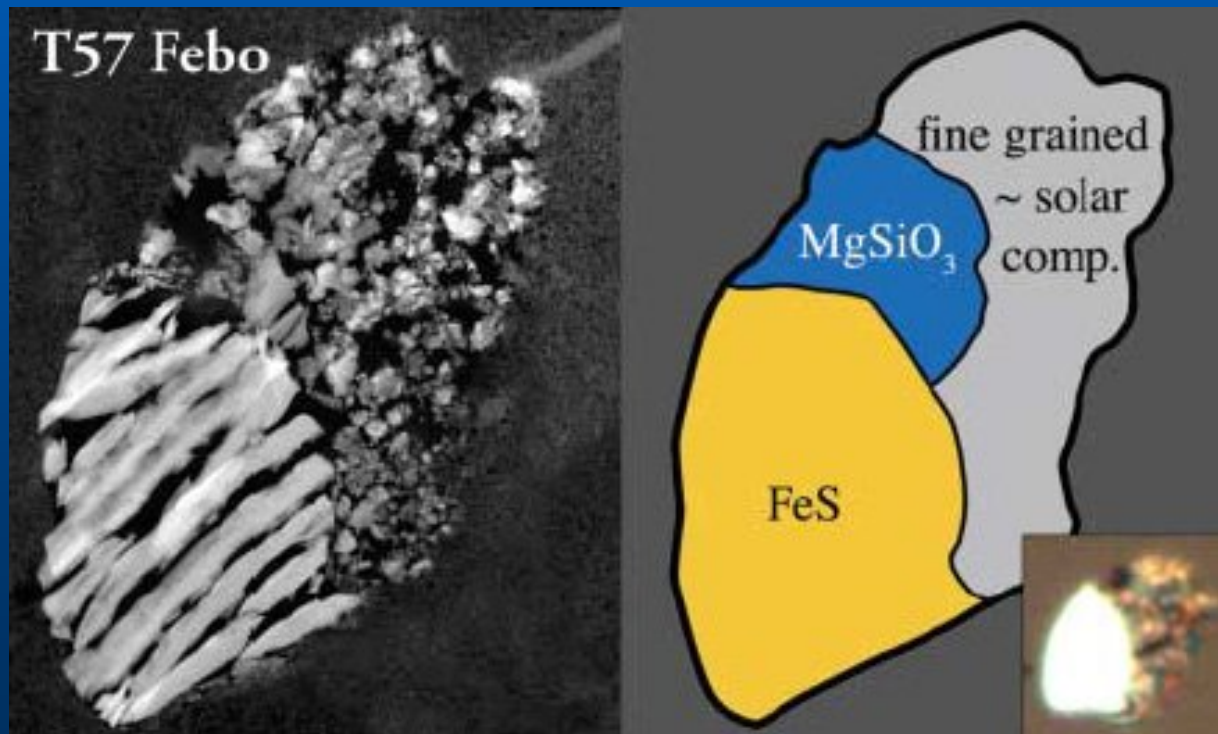
Consistent values with modeling and experiments: 1-10 kPa (Sirono, 2004; Bar-Nun et al., 2007)



Trigo-Rodriguez & Llorca (2006, 2007), MNRAS.

# THE NATURE OF 81P/WILD 2

- At microscopic scale 81P/Wild 2 is formed by fragile aggregates
  - Preferential fragmentation in the aerogel under few kPa load strengths
- The largest recovered grains by Stardust were ~5-15 $\mu\text{m}$  in diameter.
  - The toughest fragments that survived the capture process (biasing)
  - But some particles (like e.g. Febo) reveal that large grains are embedded in fragile aggregates similar to the matrix of carbonaceous chondrites, except for being highly porous



8  $\mu\text{m}$ -size particle (FEBO) (Brownlee et al., 2006)

# CONCLUSIONS

- To recover “pristine” materials from cometary surfaces can be very challenging due to the extremely low tensile strengths
  - Comets stored far away from the Sun probably have preserved their primeval physical properties due to have avoided collisional processing.
  - Future sample return missions will have the goal to collect and preserve unaltered samples of cosmochemical significance.
- A simple instrument to measure the tensile strength of granular materials:
  - The collected granular material from the surface is deposited in a cm-sized cell.
  - A TV camera records the avalanches driven by the centrifugal force.
  - A quick measurement of the material tensile strength is obtained from the analysis of these avalanches by means of image software
- Such a device would be incorporated into a small lander or an orbiting spacecraft in order to measure *in situ* the tensile strength of the surface.
  - The granular material to be tested would be collected from the surface with the help of a robotic arm. In this way, orbital maneuvers nearby the body would allow to get information on the consistence of its surface before landing.
  - A penetrator would also allow taking samples at different depths, thus having the possibility of measuring the strength of materials at deeper layers.



GOOD LUCK ROSETTA!

# Discussion

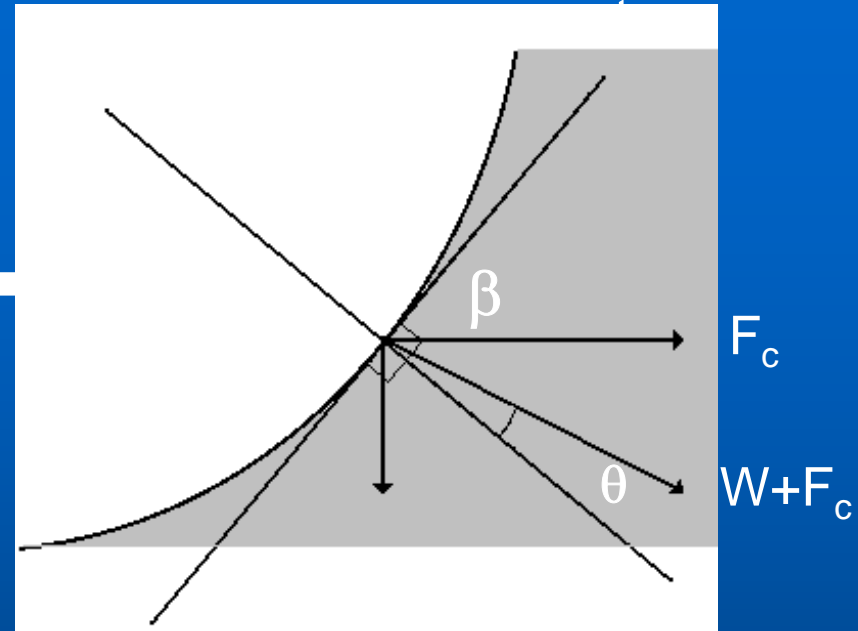
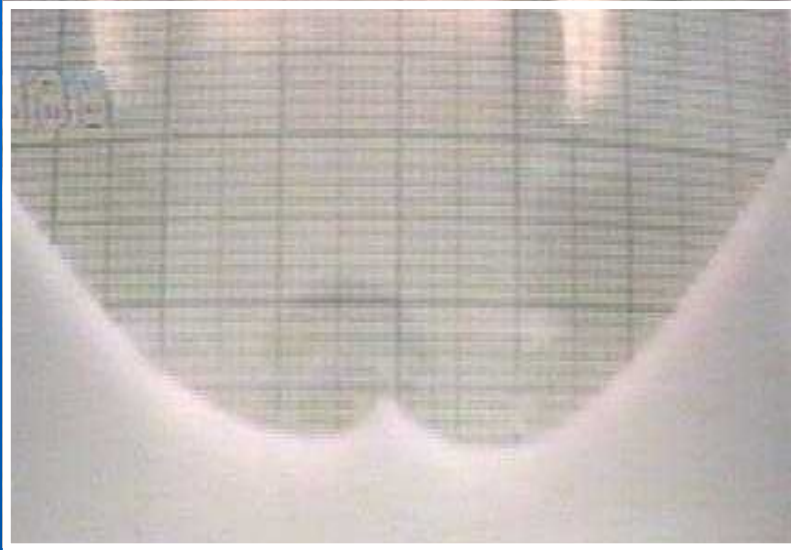
- The movement of the material up the slope is driven by the centrifugal force
- The angles  $\alpha$  and  $\theta$  are very similar. In the limit:

$$\alpha \rightarrow \theta$$

$$\frac{F_c}{W} = \frac{\omega^2 \cdot R}{g} \cdot \left(1 - \frac{2 \cdot \Delta R}{3 \cdot R}\right) = \tan \chi$$

- $\Delta R$  and  $\alpha$  are measured using an image processing program
- $\omega$  is read from the videotape
  - The angle  $\chi$  relates the centrifugal force to the weight
  - $\phi$  is obtained as a function of  $\chi$

# Behavior of non-cohesive powder



- For  $\theta < \phi$  the powder is stable
- For  $\theta = \phi$  the powder fails

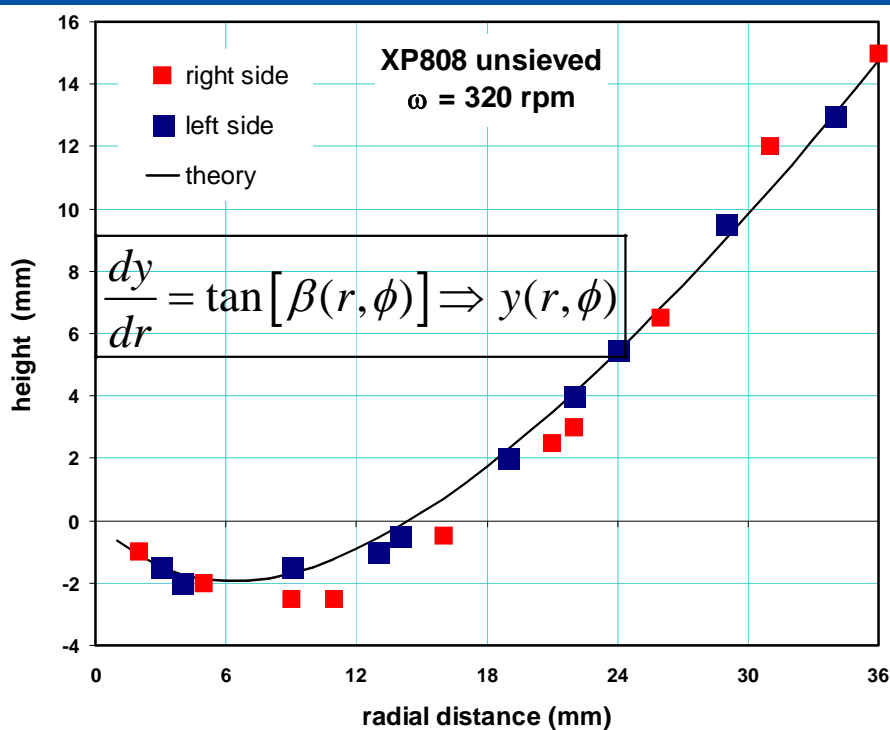
$$\frac{\tau}{\sigma} = \frac{\omega^2 r \cos(\beta) - g \sin(\beta)}{\omega^2 r \sin(\beta) + g \cos(\beta)}$$

The condition of failure reads:

$$\tan(\phi) = \frac{\tau}{\sigma}$$

Measured  $\phi = 35^\circ$

(error < 10%)



# Theoretical methodology

## Coulomb's method of wedges

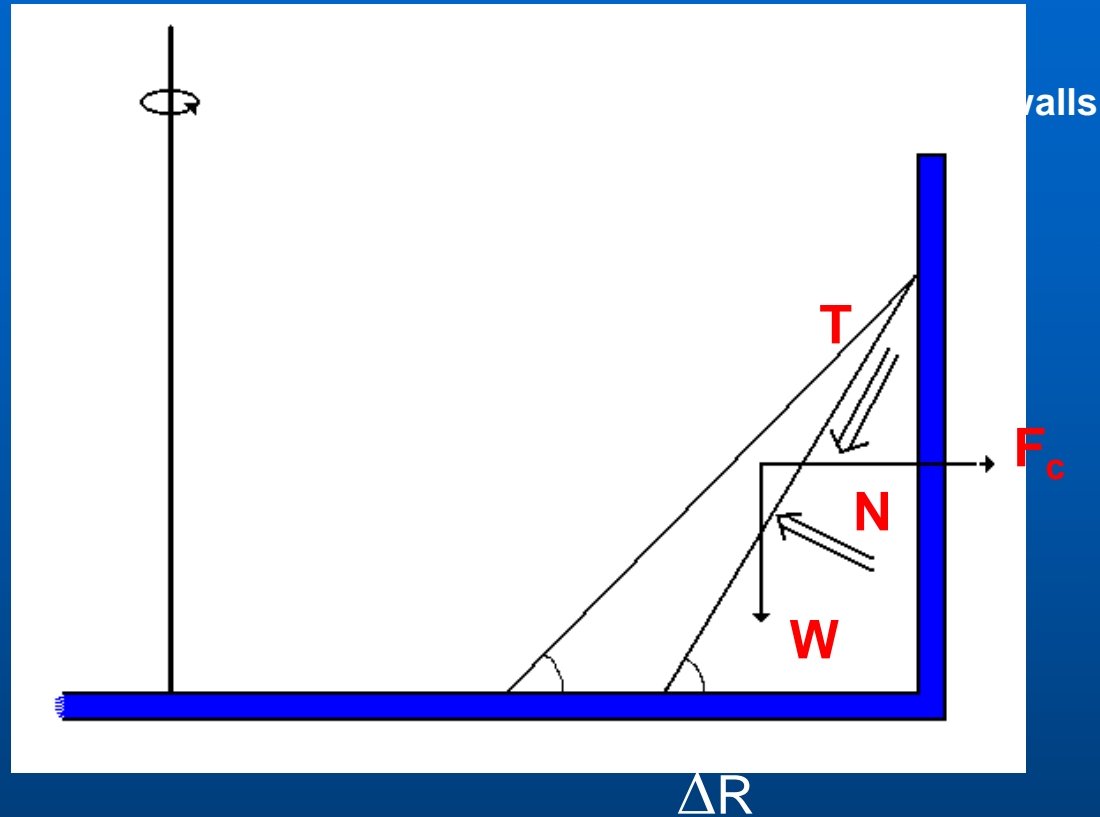
Granular materials form wedges that move as rigid solids in sliding motion

Motion starts when the **equilibrium equations of the acting forces and the Mohr-Coulomb criterion for failure in the slipping surfaces,**

$$\sum_i F_i = 0 \quad \tau_i = \sigma_i \cdot \tan \phi + c$$

**are simultaneously satisfied**

# Modeling - mathematical formulation



Equilibrium of forces

$$F_c \cdot \cos \alpha - W \cdot \sin \alpha - T = 0$$

$$F_c \cdot \sin \alpha + W \cdot \cos \alpha - N = 0$$

Mohr - Coulomb criterion

$$T \leq N \cdot \tan \phi + \frac{c \cdot h}{\cos \alpha}$$

## Determination of $\phi$

Operating, from the critical equilibrium condition, we obtain

$$\sin(\alpha - \theta) \cdot \sin[\chi - (\alpha + \phi)] \leq \frac{2 \cdot c}{\rho \cdot g \cdot h} \cdot \cos \phi \cdot \cos \chi \cdot \sin \theta$$

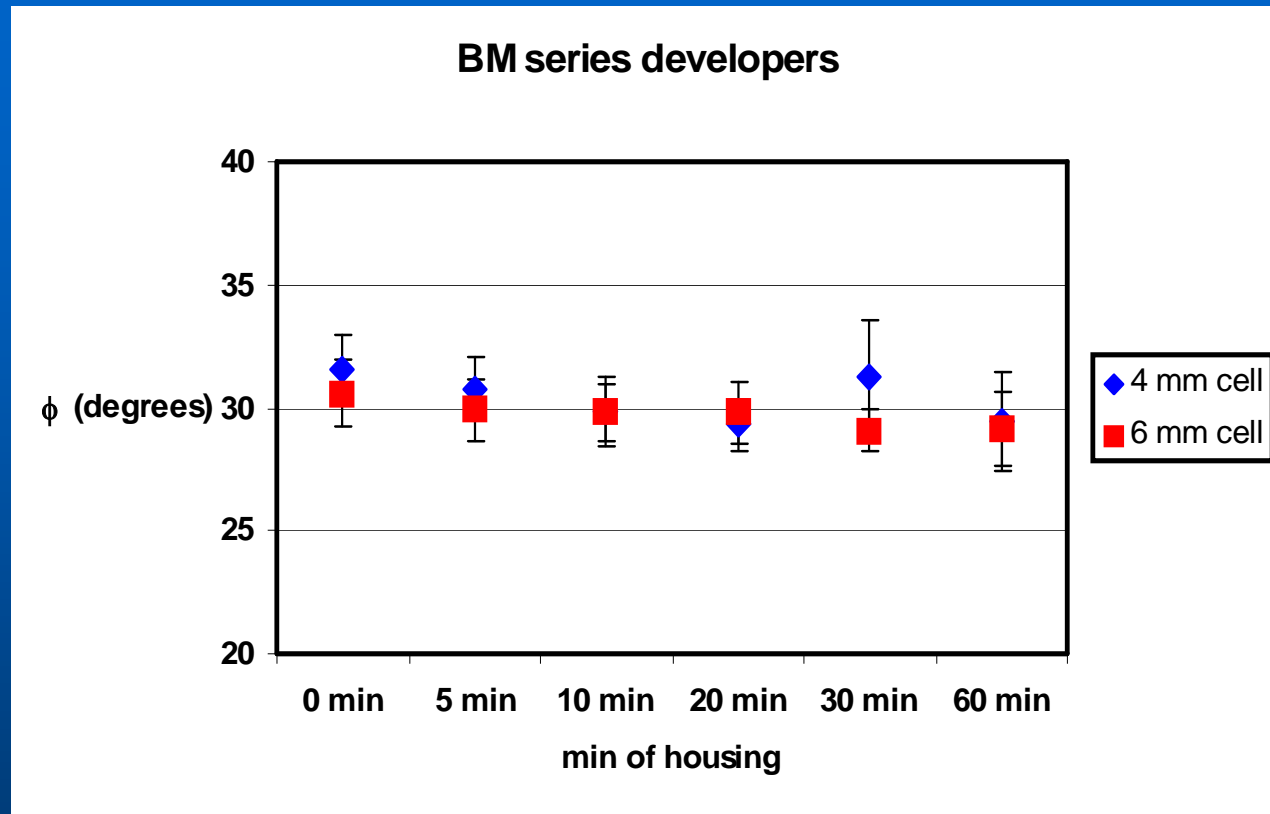
The angle that maximizes the left hand side of this equation is angle of the slope at critical equilibrium. This angle is given by:

$$\alpha = \frac{\chi - \phi + \theta}{2}$$

Since  $\alpha \sim \theta$    $\phi \approx \chi - \alpha$

where:  $\tan \chi = \frac{\omega^2 \cdot R}{g} \cdot \left(1 - \frac{2 \cdot \Delta R}{3 \cdot R}\right)$

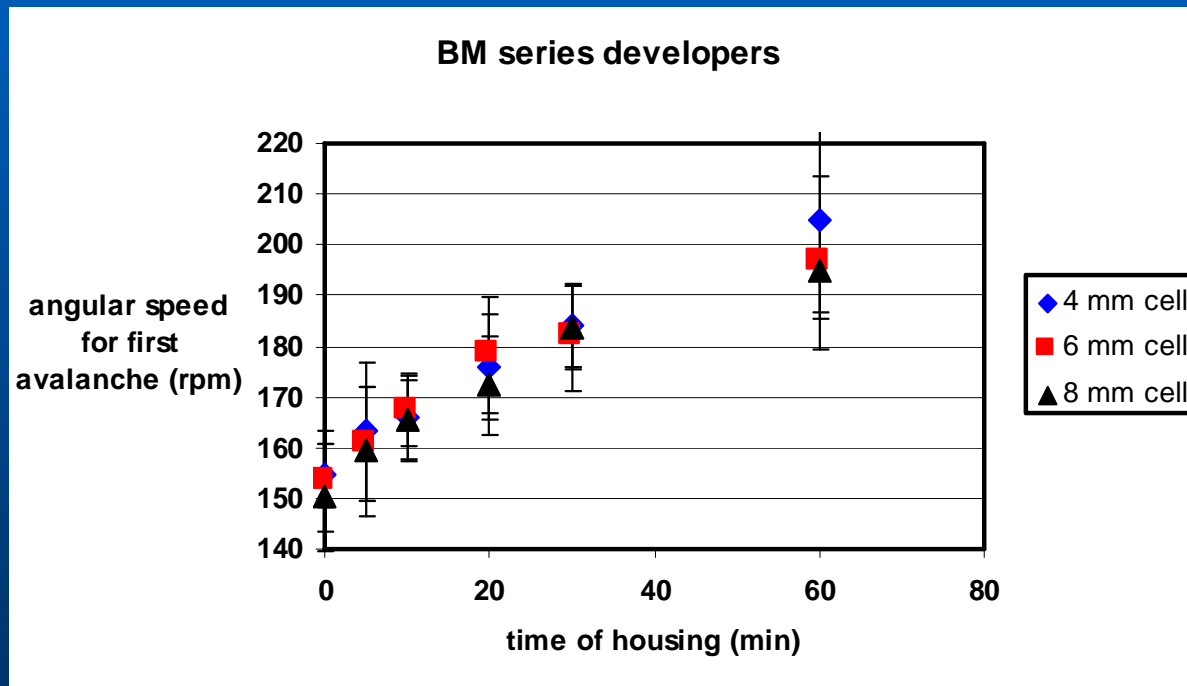
# Experimental results



- Angle of internal friction does not depend on aging
- No wall effects were observed

# Determination of cohesion

- Once we know the angle of internal friction we can proceed to find the cohesion
- Cohesion is obtained from the angular speed at which first avalanche occurs



Angular speed for first avalanche increases with aging time

# First avalanche mechanism

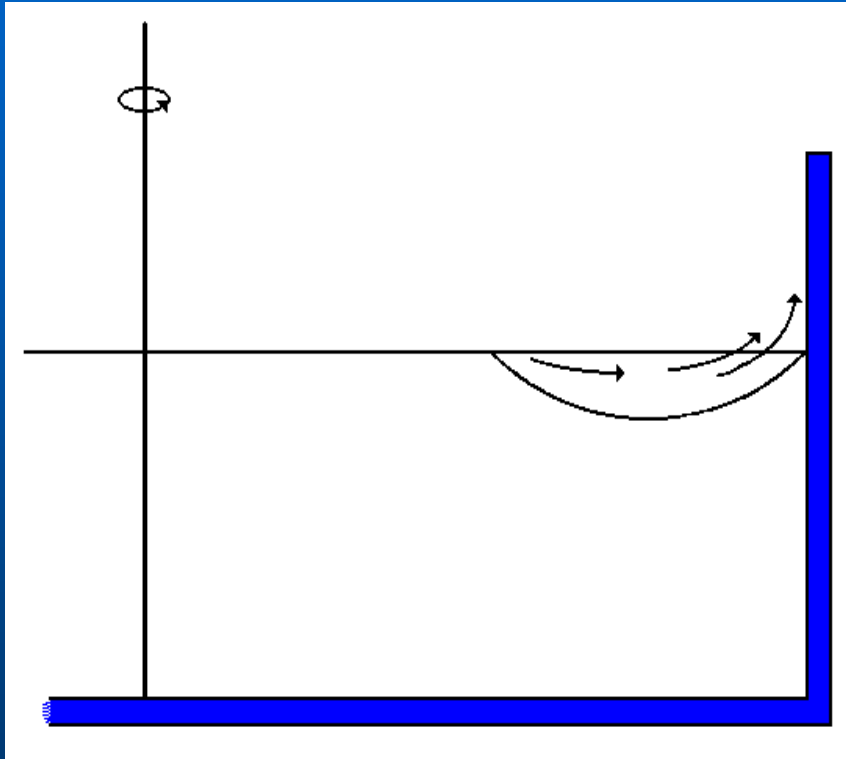


- The material suddenly fails in the outer part of the cell forming a slope
- The inner part of the sample is unaffected.

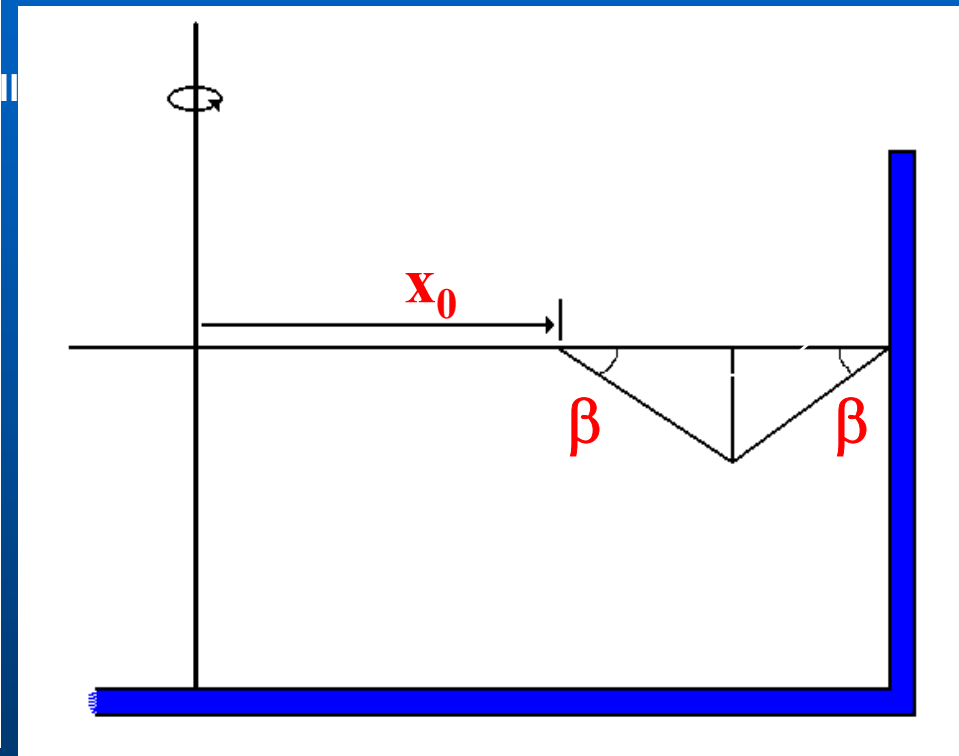
# Model for cohesive powder behavior

## Model of two wedges

The avalanche is modeled as a system of two wedges



actual wedge

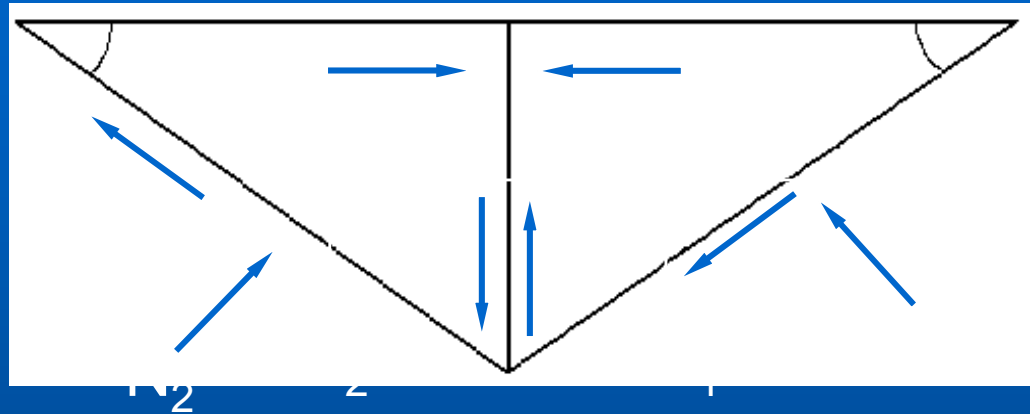
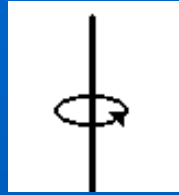


model wedges

model wedges depends on two parameters:  $\beta$  and  $x_0$

# Modeling - mathematical formulation

## Model of two wedges



### Equilibrium of forces

$$F_1 - N_1 \cdot \sin \beta - T_1 \cdot \cos \beta + N_3 = 0$$

$$F_2 - N_2 \cdot \sin \beta - T_2 \cdot \cos \beta - N_3 = 0$$

$$N_1 \cdot \cos \beta - T_1 \cdot \sin \beta - W_1 - T_3 = 0$$

$$N_2 \cdot \cos \beta + T_2 \cdot \sin \beta - W_2 + T_3 = 0$$

### Mohr - Coulomb criterion

$$0 < T_1 \leq N_1 \cdot \tan \phi + \frac{1}{2} \cdot c \cdot (R - x_0) \cdot \sec \beta$$

$$0 < T_2 \leq N_2 \cdot \tan \phi + \frac{1}{2} \cdot c \cdot (R - x_0) \cdot \sec \beta$$

$$0 < T_3 \leq N_3 \cdot \tan \phi + \frac{1}{2} \cdot c \cdot (R - x_0) \cdot \tan \beta$$

# Theoretical results for the first avalanche

## Model of two wedges

Using the Mohr-Coulomb criterion with sign = (slipping), and solving for  $\omega$  we find:

$$\Omega = \frac{f_1(\beta, \phi) + \frac{24 \cdot \gamma}{1 - \zeta} \cdot f_2(\beta, \phi)}{(2 + \zeta) \cdot f_3(\beta, \phi) + (1 + 2 \cdot \zeta) \cdot f_4(\beta, \phi)}$$

$$f_1(\beta, \phi) = 6 \sin(\phi) [\cos(2\phi) + \sin^2(\beta)]$$

$$f_2(\beta, \phi) = \frac{\cos(\phi) \cos(\beta)}{\sin(\beta)} [\cos(2\phi) + \sin^2(\beta)]$$

$$f_3(\beta, \phi) = \cos(\beta + \phi) \cos(\beta - 2\phi)$$

$$f_4(\beta, \phi) = \cos(\beta - \phi) \cos(\beta + 2\phi)$$

where:

$$\Omega = \frac{\omega^2 \cdot R}{g}$$

Ratio between centrifugal acceleration and gravity.

$$\zeta = \frac{x_0}{R}$$

Distance to center at which avalanche occurs, measured in units of R.

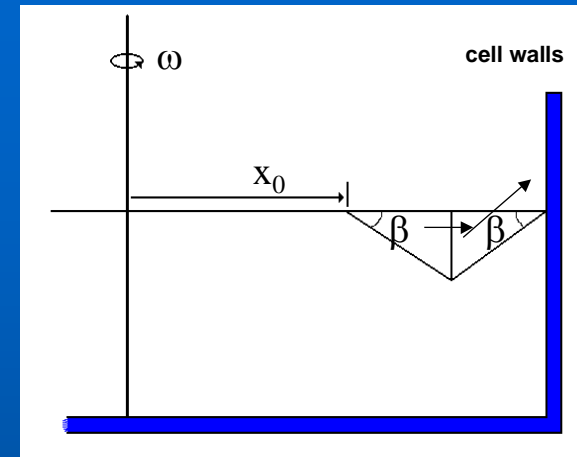
$$\gamma = \frac{c}{\rho \cdot g \cdot R}$$

Ratio between cohesion and consolidation.

For a cohesive powder ( $\gamma \neq 0$ ), if  $\zeta \rightarrow 1$  then,  $\Omega \rightarrow \infty$ , therefore a cohesive powder cannot move grain by grain

# Numerical results for cohesion $\omega = \omega(x_0, \beta, c, \phi)$

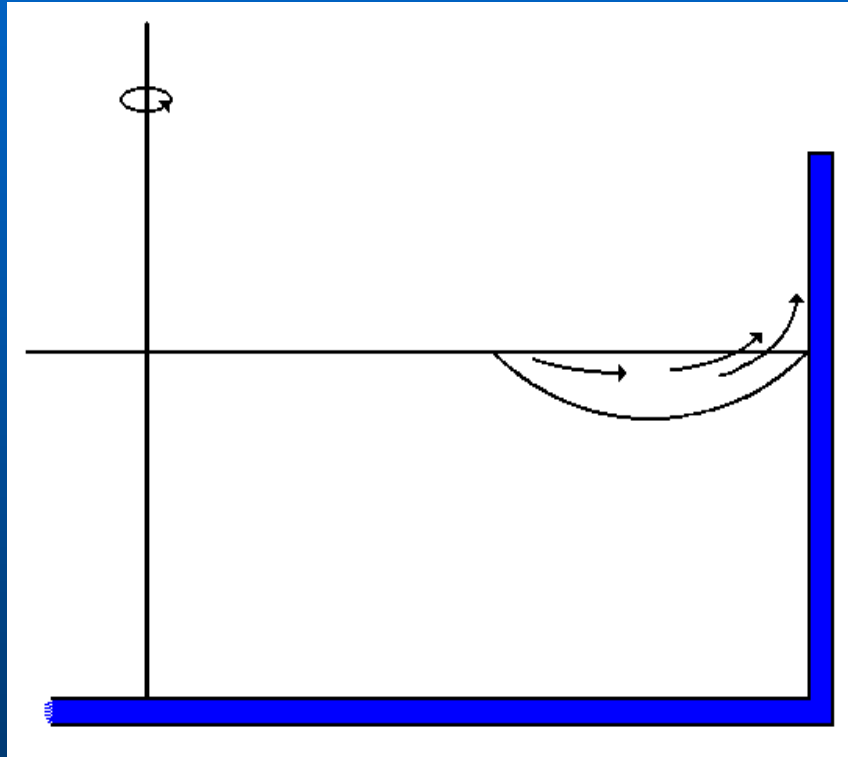
- The minimum of  $\Omega$  with the condition that  $N_3 > 0$  and  $T_3 > 0$  gives the angular speed at which first avalanche takes place if the cohesion is known
- A table showing the value of the minimum of  $\Omega$  for every value of the cohesion. The minimum of  $\Omega$  is forced to match the experimentally measured  $\Omega$  at breaking.
- Obtain the value of the cohesion from the table, inspecting the row that corresponds to the angle of internal friction of the powder previously obtained and to the experimental  $\Omega$  at breaking



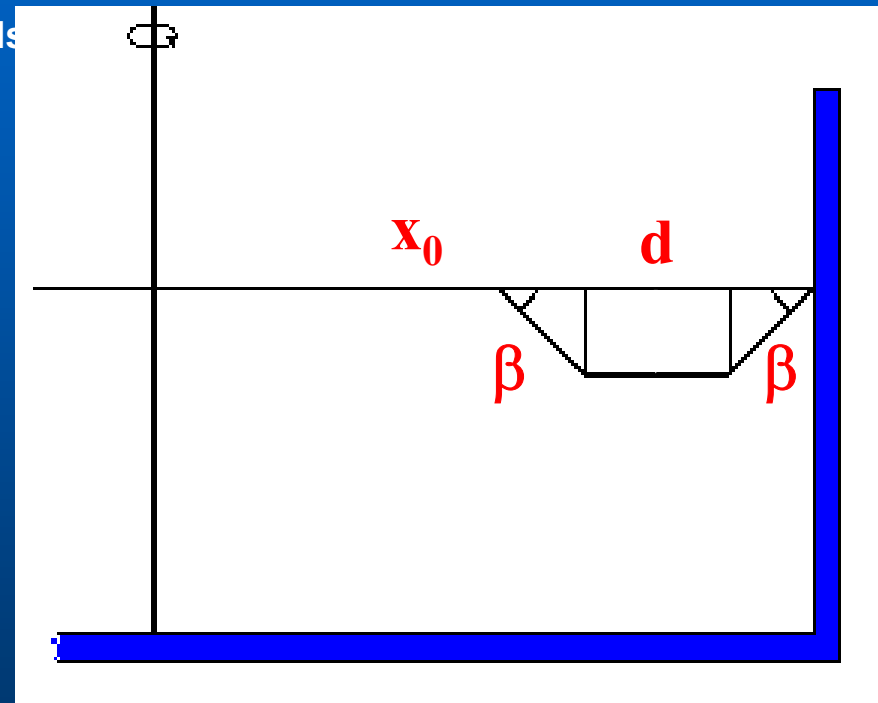
	$\gamma$	0.001	0.002	0.003	0.004	0.005	0.006	0.007	0.008	0.009	0.010	0.011	0.012	0.013	0.014
$\phi$ (degrees)															
25		0.694	0.786	0.857	0.921	0.981	1.033	1.083	1.132	1.179	1.225	1.268	1.309	1.350	1.391
26		0.724	0.817	0.892	0.957	1.017	1.073	1.124	1.173	1.221	1.267	1.313	1.357	1.398	1.439
27		0.754	0.849	0.928	0.993	1.055	1.113	1.166	1.216	1.264	1.312	1.358	1.403	1.448	1.491
28		0.784	0.882	0.964	1.031	1.094	1.152	1.209	1.261	1.310	1.358	1.405	1.451	1.497	1.541
29		0.814	0.917	0.999	1.071	1.135	1.194	1.251	1.307	1.359	1.408	1.455	1.501	1.547	1.592
30		0.846	0.953	1.036	1.112	1.178	1.238	1.296	1.352	1.406	1.460	1.508	1.555	1.601	1.647
31		0.878	0.991	1.075	1.152	1.223	1.285	1.343	1.400	1.455	1.509	1.561	1.613	1.660	1.706
32		0.913	1.028	1.116	1.194	1.266	1.334	1.394	1.451	1.507	1.561	1.615	1.667	1.718	1.769
33		0.949	1.065	1.160	1.238	1.311	1.380	1.447	1.506	1.563	1.618	1.672	1.724	1.776	1.828
34		0.987	1.105	1.205	1.286	1.360	1.430	1.497	1.562	1.624	1.679	1.734	1.787	1.840	1.891
35		1.024	1.147	1.248	1.338	1.413	1.484	1.552	1.617	1.681	1.743	1.802	1.857	1.909	1.962
36		1.062	1.193	1.295	1.387	1.472	1.543	1.612	1.678	1.742	1.804	1.866	1.926	1.985	2.040
37		1.102	1.243	1.346	1.439	1.525	1.607	1.679	1.746	1.810	1.873	1.935	1.995	2.055	2.113
38		1.146	1.291	1.403	1.497	1.583	1.666	1.745	1.821	1.888	1.952	2.014	2.074	2.134	2.193
39		1.194	1.341	1.464	1.563	1.650	1.733	1.812	1.888	1.962	2.035	2.105	2.166	2.225	2.284
40		1.250	1.397	1.521	1.632	1.729	1.812	1.891	1.967	2.040	2.112	2.182	2.251	2.319	2.386

# Model for cohesive powder behavior

## Model of three wedges



actual wedge

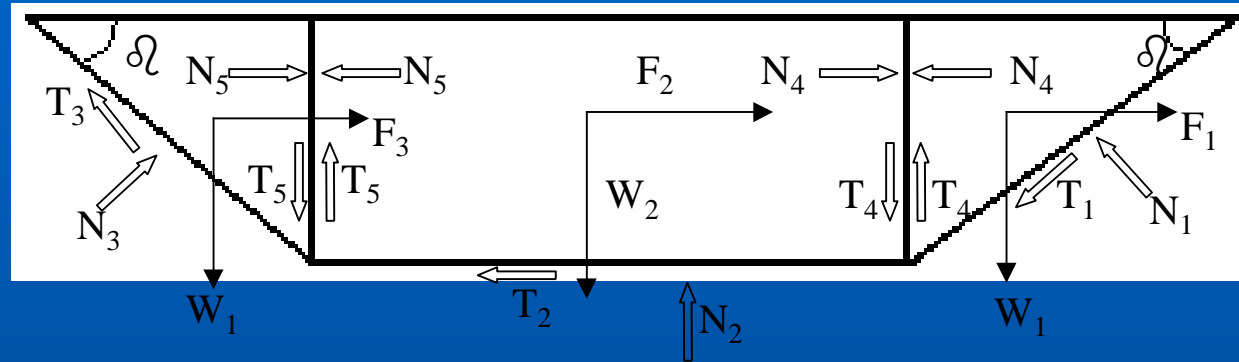
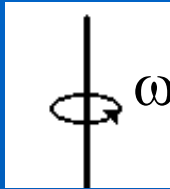


model wedges

model wedges depends on two parameters:  $\beta$ ,  $d$  and  $x_0$

# Modeling - mathematical formulation

## Model of three wedges



### Equilibrium of forces

$$F_1 + N_4 - N_1 \sin(\beta) - T_1 \cos(\beta) = 0$$

$$F_3 - N_5 + N_3 \sin(\beta) - T_3 \cos(\beta) = 0$$

$$F_2 + N_5 - N_4 - T_2 = 0$$

$$W_1 + T_4 - N_1 \cos(\beta) + T_1 \sin(\beta) = 0$$

$$W_2 + T_5 - T_4 - N_2 = 0$$

$$W_1 + T_5 - N_3 \cos(\beta) - T_3 \sin(\beta) = 0$$

### Mohr - Coulomb criterion

$$T_1 = N_1 \tan(\phi) + \frac{cs}{\tan(\beta)}$$

$$T_2 = N_2 \tan(\phi) + c \left[ (R - x_0) - \frac{2s}{\tan(\beta)} \right]$$

$$T_3 = N_3 \tan(\phi) + \frac{cs}{\tan(\beta)}$$

$$T_4 = N_4 \tan(\phi) + cs$$

$$T_5 = N_5 \tan(\phi) + cs$$

# Theoretical results for the first avalanche

## Model of three wedges

Solving for  $\omega$  as we did for two blocks we find:

$$\Omega = \frac{\delta \frac{\sin(\phi)}{\cos(2\phi)} \left[ (1-\zeta) - \frac{2\delta}{\tan(\beta)} \right] + \frac{\delta^2}{2\tan(\beta)} f(\beta, \phi) + \gamma \delta g(\beta, \phi) + \gamma \frac{\cos(\phi)}{\cos(2\phi)} \left[ (1-\zeta) - \frac{2\delta}{\tan(\beta)} \right]}{\frac{\delta^2}{2\tan(\beta)} \frac{\cos(\beta+\phi)}{\cos(\beta+2\phi)} \left[ 1 - \frac{2\delta}{3\tan(\beta)} \right] + \frac{\delta}{2} \frac{\cos(\phi)}{\cos(2\phi)} \left[ 1 - \zeta^2 - \frac{2\delta}{\tan(\beta)} (1+\zeta) \right] + \frac{\delta^2}{2\tan(\beta)} \frac{\cos(\beta-\phi)}{\cos(\beta-2\phi)} \left[ \zeta + \frac{2\delta}{3\tan(\beta)} \right]}$$

where:

$$g(\beta, \phi) = \frac{\cos(\phi)}{\sin(\beta)} \left[ \frac{1}{\cos(\beta-2\phi)} + \frac{1}{\cos(\beta+2\phi)} \right] + \left[ \frac{\sin(\beta+\phi)}{\cos(\beta+2\phi)} + \frac{\sin(\beta-\phi)}{\cos(\beta-2\phi)} \right]$$

$$f(\beta, \phi) = \frac{\sin(\beta+\phi)}{\cos(\beta+2\phi)} - \frac{\sin(\beta-\phi)}{\cos(\beta-2\phi)}$$

$$\Omega = \frac{\omega^2 \cdot R}{g}$$

Ratio between centrifugal acceleration and gravity.

$$\zeta = \frac{x_0}{R}$$

Distance to center at which avalanche occurs, measured in units of R.

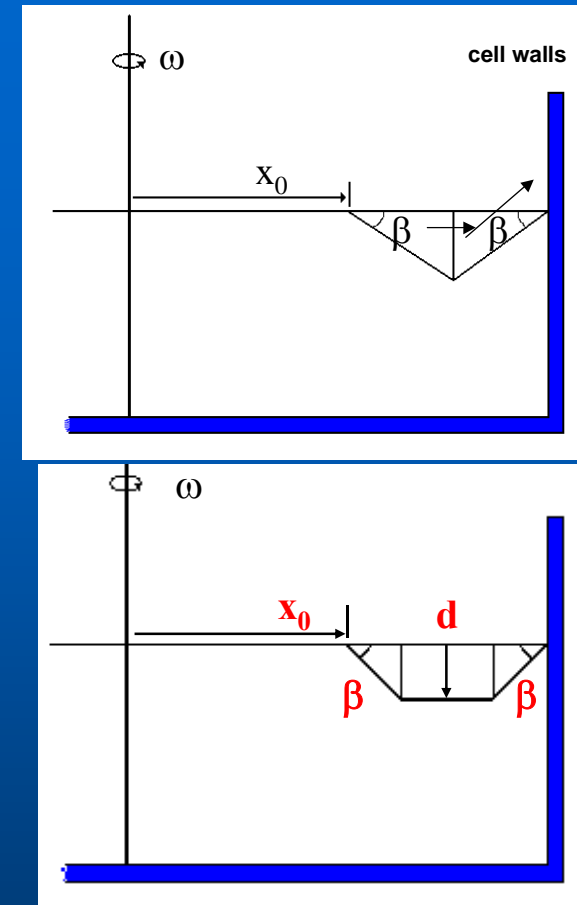
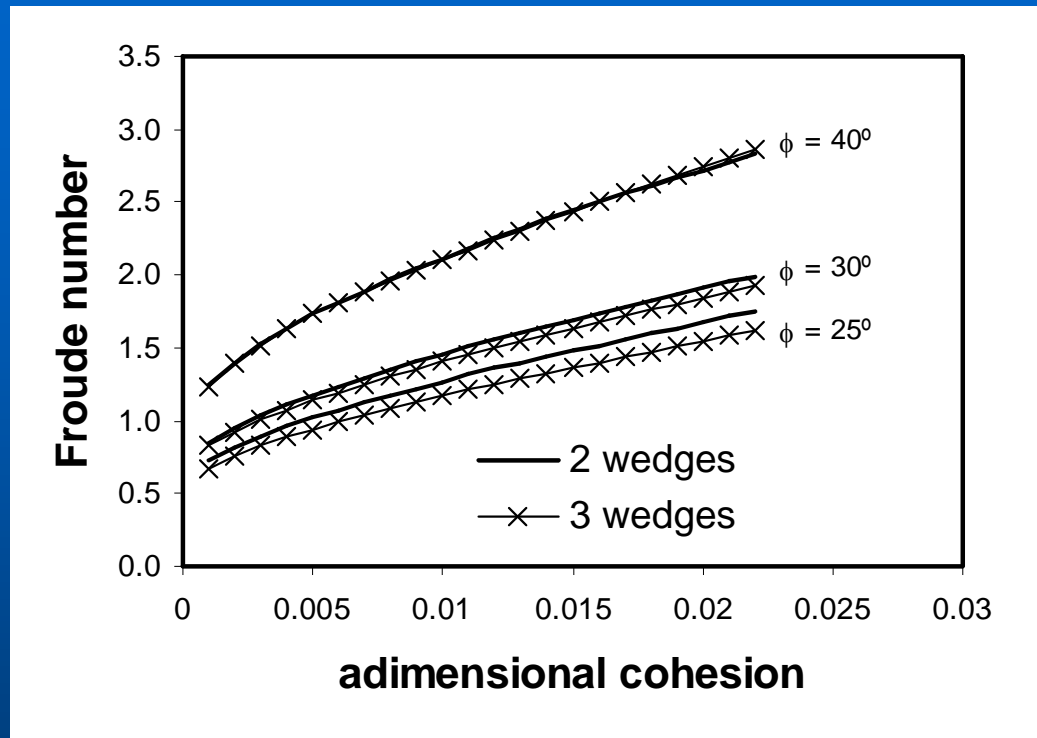
$$\gamma = \frac{c}{\rho \cdot g \cdot R}$$

Ratio between cohesion and consolidation.

$$\delta = \frac{d}{R}$$

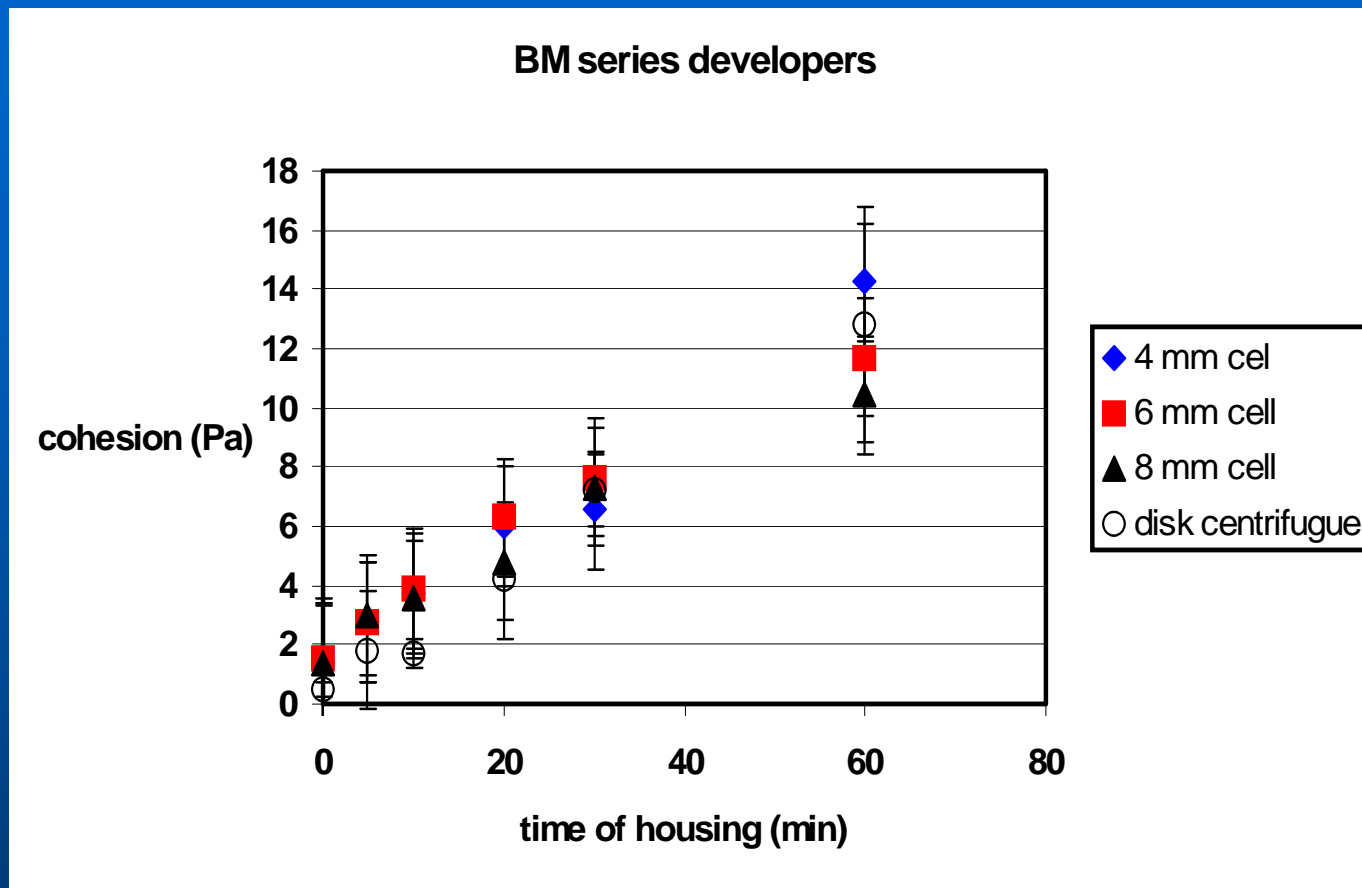
Avalanche depth.

# Numerical results for cohesion



- The highest difference between results of the two models is of the order of 5%.
- As the experimental scatter of the data is larger than this, it is not worthy using three or more wedges

# Experimental results for cohesion



- Cohesion increases with aging time
- No wall effects were observed
- Results are consistent with former results

# Conclusions

- A novel technique for determining powder flow of cohesive powders
- Advantages of this technique:
  - It is possible to measure both angle of internal friction and cohesion in the same experiment
  - The experiment needs only a small quantity of material
  - Time to run the experiment is short
- Experiment is being automated
- Pre-conditioning procedure must be incorporated